

# Optimization of Estimation Parameters for Shambesai Gold Deposit in Kyrgyzstan

Huaming An, Song Huang \*

**Abstract**—Geostatistics was applied for the parameters optimization in the estimation process for the Shambesai gold deposit in Kyrgyzstan. Surpac and Supervisor were used as the main geostatistics analysis and block model estimation software. Referring to the characteristics of the mineralization type of the Carlin gold deposit, parameter optimization methods were used at different stages of estimation: the sampling spacing, top-cut, proportional effect and mixed distribution were researched for creating robust experimental variogram; logarithmic model was used for model fitting and zonal nesting method was applied to calculate the best fitting variogram fitting curves; parameters of slope of regression, Kriging efficiency and block variance were used for the optimization of block model estimation parameters, and finally the resource was completed with reasonable setting and best accuracy.

**Index Terms**—Geostatistics, Ordinary Kriging, experimental variogram, zonal nesting, SR and KE indicator

## I. INTRODUCTION

Matheron G, a famous French statistician, firstly proposed the concept of geostatistics in the book of “*Traité de géostatistique appliquée*”, Professor Matheron put forward the concept of regionalized variables and established the discipline of geostatistics. Geostatistics is a science based on regionalized variables and uses variation functions as a tool to study the natural phenomena of both randomness and designability, or spatial correlation and dependence. The theory and method of geostatistics can be applied to the study of the spatial data's randomness and designability, or spatial correlation and dependence, or the study of spatial pattern and variation, and the optimal unbiased interpolation estimation of these data, or the discreteness and volatility of data. According to the theory of geostatistics, geological characteristics can be characterized by the spatial distribution characteristics of regionalized variables. The main mathematical tool for studying the spatial distribution characteristics of regionalized variables is the variogram [1-2]. The estimation methods of geostatistics include simple Kriging, ordinary Kriging, universal Kriging, co-Kriging, and indicator Kriging.

Since 1990s, a large number of three dimensional geological software based on Geostatistics has been

developed globally. The theory of geostatistics has gradually become mature while the computer technology has unprecedented development as well. Meanwhile, the geostatistics analysis and commercial software have sprung up such as IDRISI, GEO-EAS, GS+, Surfer, GeoDA, Surpac, Datamine, and Vulcan etc.

In this study, the Surpac mining software was used to construct a three dimensional model of a gold mine in Kyrgyzstan and supervisors software was used as main geostatistic analysis tools. The sampling spacing, top-cut, proportional effect and mixed distribution were researched for creating robust experimental variogram; logarithmic model was used for model fitting and zonal nesting method was applied to calculate the best fitting variogram fitting curves; a series of Kriging parameters were used for the optimization of block model estimation parameters, and finally the resource was completed with reasonable setting and best accuracy.

## II. GEOLOGY OF STUDY AREA

The Turkestan-Alai and Southern Fergana (or Aravan) Segments of the Western Southern Tianshan form the EW trending mountains of Southwest Kyrgyzstan (Figure 1), stretching about 400 km long and 50km wide. They are made up of fold-and-thrust belts of fore-arc accretionary complexes, passive continental slope sediments and minor volcanics.

They formed during the Hercynian Orogeny from the Ordovician to Upper Carboniferous as the Turkestan Ocean closed between the Alai-Tarim microcontinent and Kazakh continent.

Three significant intrusive groups occurred in the Southern Tianshan. Two of these are the syn-collisional (gabbro-monzodiorite-granite suite) and a post-collisional (A-type granites, granosyenites, alaskites, monzonites and syenites) intrude the Turkestan-Alai segment. The entire Southern Tianshan was a stable continental area until India collided with Asia from the Miocene to the present, creating the Southern Tianshan's current height and orientation.

The Shambesai ore body strikes ENE for 1.4km, at most part is 300m wide and 30m thick. Gold ore occurs primarily in a sub-horizontal ‘trough’ or step, on the contact formed by pre or syn-mineralization deformation. The tectonic breccia within this step is the primary host of Au mineralization. Un-brecciated siltstone does carry mineralization, but only when proximal to a brecciated zone. Organic carbon is common in the upper siltstone. Limestone blocks, interpreted as possible debris from the reef-front, occur within the siltstone and also host mineralization at their boundary.

Manuscript received Aug. 11, 2018; revised May 11, 2019.

Huaming An, is with the Faculty of Public Security and Emergency Management, Kunming University of Science and Technology, 650093, Kunming, China. (huaming.an@yahoo.com)

\*Corresponding author: Song Huang is with the University of Science & Technology Beijing, 100083, China (e-mail: shuang@rmpglobal.com).

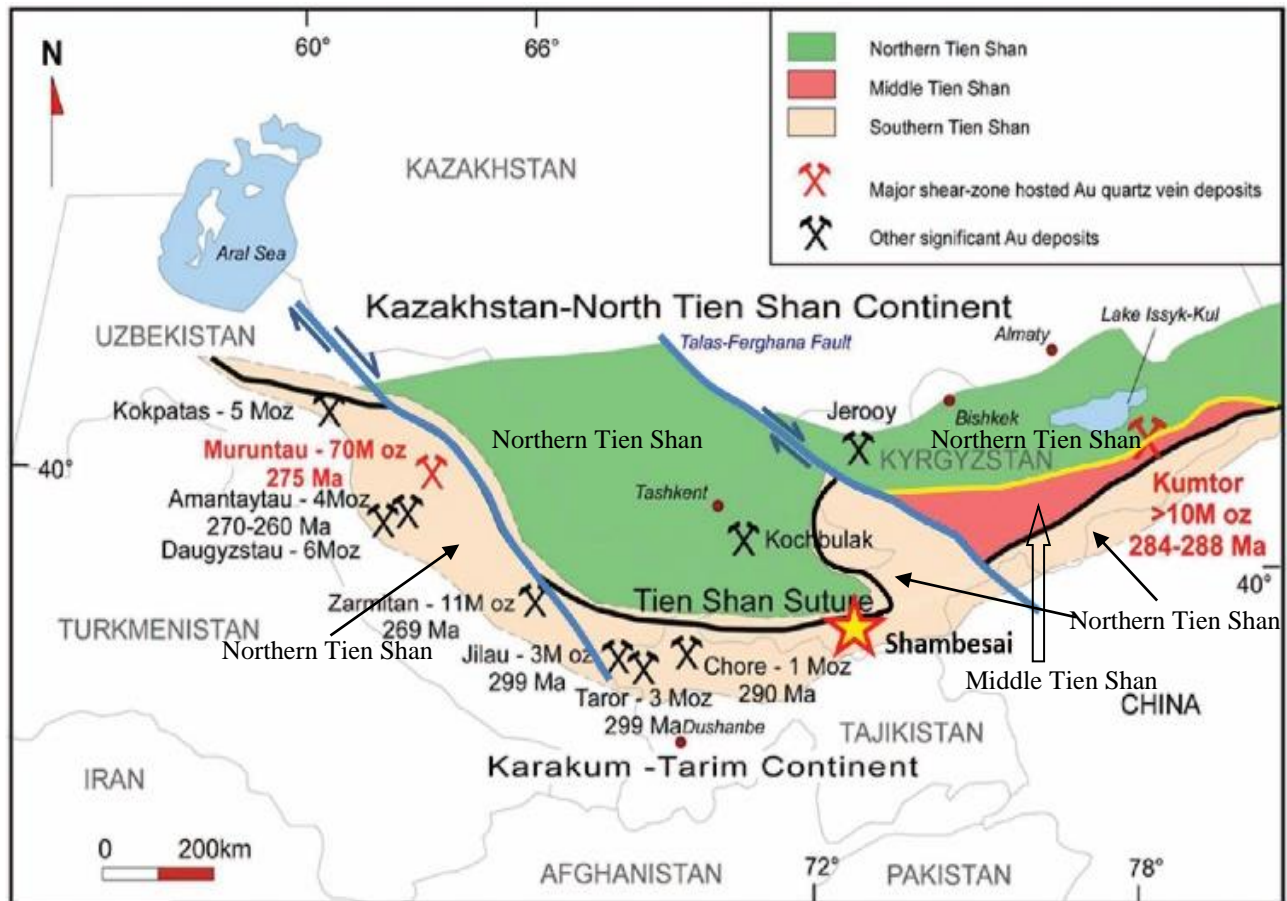


Fig.1. Shambesai Au deposit regional geology map

Massive limestone is barren except where strongly brecciated <1m from the contact. Notably, the oxidation profile is inverted so that sulfide ore occurs above oxide ore, which is invariably found at the limestone contact. Oxide ore has been found in the deepest drilling at a depth 409m. This is probably due to meteoric water flowing along the contact.

### III. CONCEPTS OF VARIOGRAM

In order to make up for the defect that classical statistics does not take into account of the spatial position of samples, the variogram is introduced into geostatistics. It can reflect the spatial variation characteristics of regionalized variables, especially reflecting the structure of regionalized variables through randomness. Variogram analysis is the basis of Kriging estimation, and its effect directly affects the accuracy of resource estimation of various methods. The calculation and fitting of the variation function mainly involve three main steps of the experimental variation function calculation. The theoretical model is used to fit the variogram of different directions or scales by fitting the variogram of different directions to the structural nesting of the variogram in different directions.

The specific definition of the variogram is that: A regionalized variable is defined as a random function in a three-dimensional. Considering a separation vector  $h$  defined by an anisotropic distance and direction (two directions, usually defined by azimuth and inclination from horizontal). The spatial variability for  $h$  is represented by the semi-variogram:  $\gamma(h)$ . The variogram is defined as the half

expected squared difference for the random variable at data points separated by  $h$ , and the variogram is experimentally estimated using the  $N(h)$  data separated by  $h$  within some defined tolerance:

$$\gamma(h) = \frac{1}{2N(h)} \sum_{i=1}^{N(h)} [z(x_i) - z(x_i + h)]^2 \quad (1)$$

In the above formula,  $N(h)$  is total number of sample pairs with  $h$  as distance;  $z(x_i)$  and  $z(x_i + h)$  are two sampling locations with  $h$  distance between each.

The variation function has the following properties:

(1) Continuity: with the increase of search distance  $h$ , the variance of the increment between the regionalized variables  $z(x_i)$  and  $z(x_i + h)$  increases gradually, and the values of the variogram curve is gradually increased from 0 value to certain values. These results show the continuity of the value of regionalization variables, such as the grade of ore body and the uniform change of thickness. If the mineralized continuity of the ore body is better in a small distance (smaller  $h$ ), the corresponding value is small, and with the increase of  $h$  value, the mineralization continuity of the ore body and the correlation becomes weaker gradually, which leads to the increase of the  $\gamma(h)$  value.

(2) Transitivity: in the usual case, when the sampling interval is greater than a certain value  $a$ , the value of the variogram will no longer increase, but is stable near a certain limit value. This value is called as "sill value" of the variogram, which is called the  $C$ , and  $a$  is the variogram distance of the experimental variogram. The sill reflects the

variability of regionalized variables. At the same time, the limit value is also a priori variance of random function, which is recorded as  $\sigma^2$ .

(3) The range of sample impact: the distance  $a$  is regarded as the range of sample impact. Regionalization variables have a certain spatial correlation with the samples in the surrounding area. The correlation decreases with the increasing distance between two points. At that time, when  $h$  is more than  $a$ , the effect between the samples disappeared.

(4) Nugget effect: even the distance of 2 points is approaching the 0 value infinitely, there is still a difference in grade between them. This phenomenon is called nugget effect in geostatistics. The nugget effect is caused by observations, analysis errors and minor changes in mineralization. The value is called nugget, expressed in  $C_0$ .

The mathematical model of spatial structure of data is obtained through the calculation of variogram and structure analysis of regionalized variables, which is a difficult and accurate points to be accurately mastered in the practical application process of the resource estimation method of geostatistics resource. In particular, how to determine the parameters to get the robust variogram, how to obtain the structural information of the regionalized variables from the variogram, and how the regionalized variables are nested when they are anisotropic structures. The above problems will be discussed in detail in this paper based on collected data from experimental gold deposits.

#### IV. EXPERIMENTAL VARIOGRAM IMPACT FACTORS

##### A. Analysis of sampling interval factors impact

The sampling interval has a direct effect on the stability of variogram. Theoretically speaking, the smaller sampling intervals chosen, the more detailed the geological information would be retained, and the more complex the curve of the variogram would be. And the too complex variogram curve can reflect the spatial variability of the sample completely, but the curve trend is not stable enough for trend definition and proper fitting. The smaller sampling intervals are chosen, the simpler the geological information can be retained, the more simplified the curve of the variogram, but too simplified variogram curve may not be effective for guiding the fitting of the variogram curve because of the factors such as excessive smoothness or hole effects. Therefore, in this paper we used the analysis method of variance and variability of the original sample data, and evaluates the robustness of the variogram through the change comparison diagram of the mean value, variance and coefficient of the variogram value. A set of stable experimental variogram curves should have smaller variance and coefficient of variation. Taking the overall data of Shambesai deposit as an example, the process of determining the sampling interval in each ore deposit area was researched [3]. Ten figures were created by different sampling intervals as below Figure 2 and Table 1.

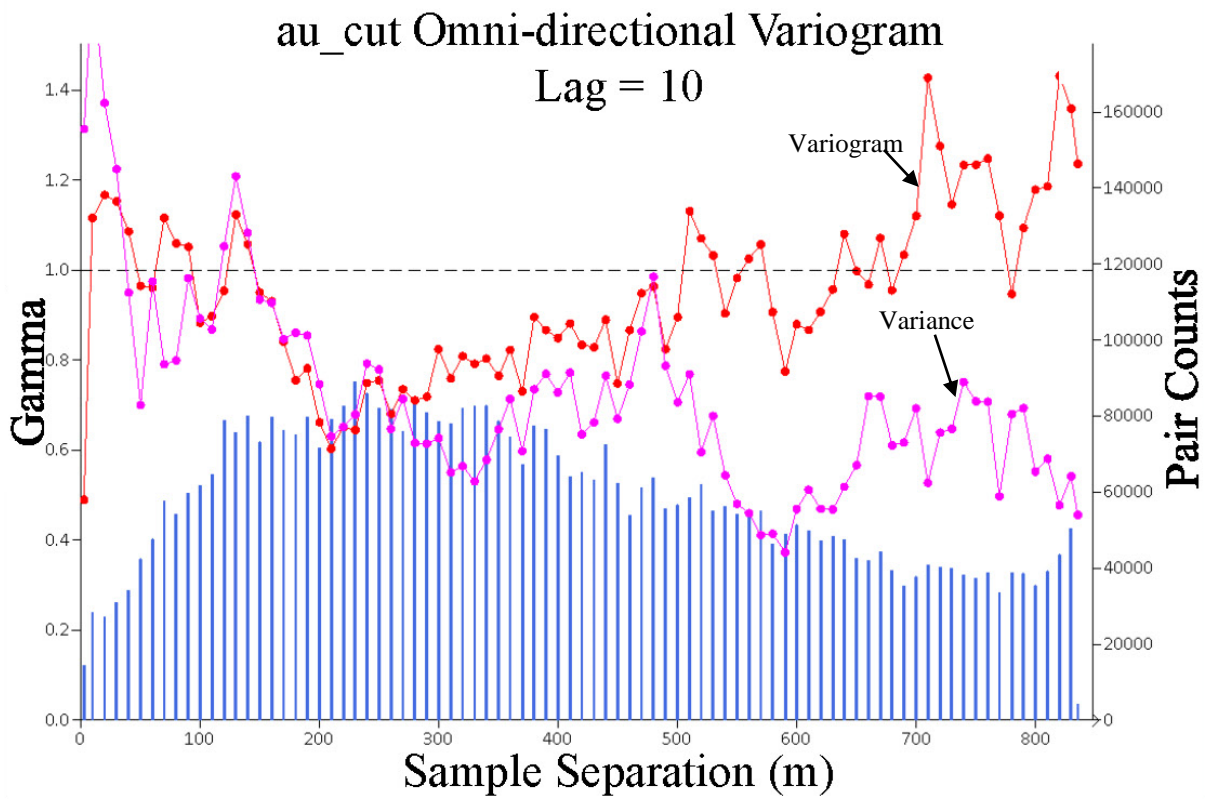
By comparison of variogram, it is found that the variability of omnidirectional variogram decreases with the increase of sampling interval. It is embodied as ten groups of

omnidirectional variogram comparison figures which include basic data statistics, trend curves of mean, variance and coefficient of variation (Figure 3). With the increasing of the sampling intervals, the standard deviation, variance and the coefficient of variation decrease gently before the interval is less than 50m. It indicates that the stability of the curve is rising gradually. Between the interval of 55m and 70m, the curve has two inflection points successively. The curve after the first 50m inflection point appears increasing trend briefly and then drops rapidly at the second 70m inflection point; at 70m location and even larger intervals, the curve drops to a certain level and then gradually becomes stable. Through the analysis of the characteristics of the figures, we can conclude that the stability of the variogram is relatively best when the sampling interval is between 40m-50m. The main reason is that the exploration interval of most of the exploration projects in the mining area is 40m×40m-50m×50m. When the search interval is close to the actual exploration spacing, the stability of the whole variance curve is influenced by the uncertainty of the local area spacing. And the relative stable and robust curves can be obtained when the step size is greater than 70m, but excessive search interval will also cause excessive smoothing of data and elimination of the local variability of ore deposits. Considering comprehensively, the general search interval of 50m being used as the experimental variogram of ore body is the most reasonable.

##### B. Analysis of sample composite length impact

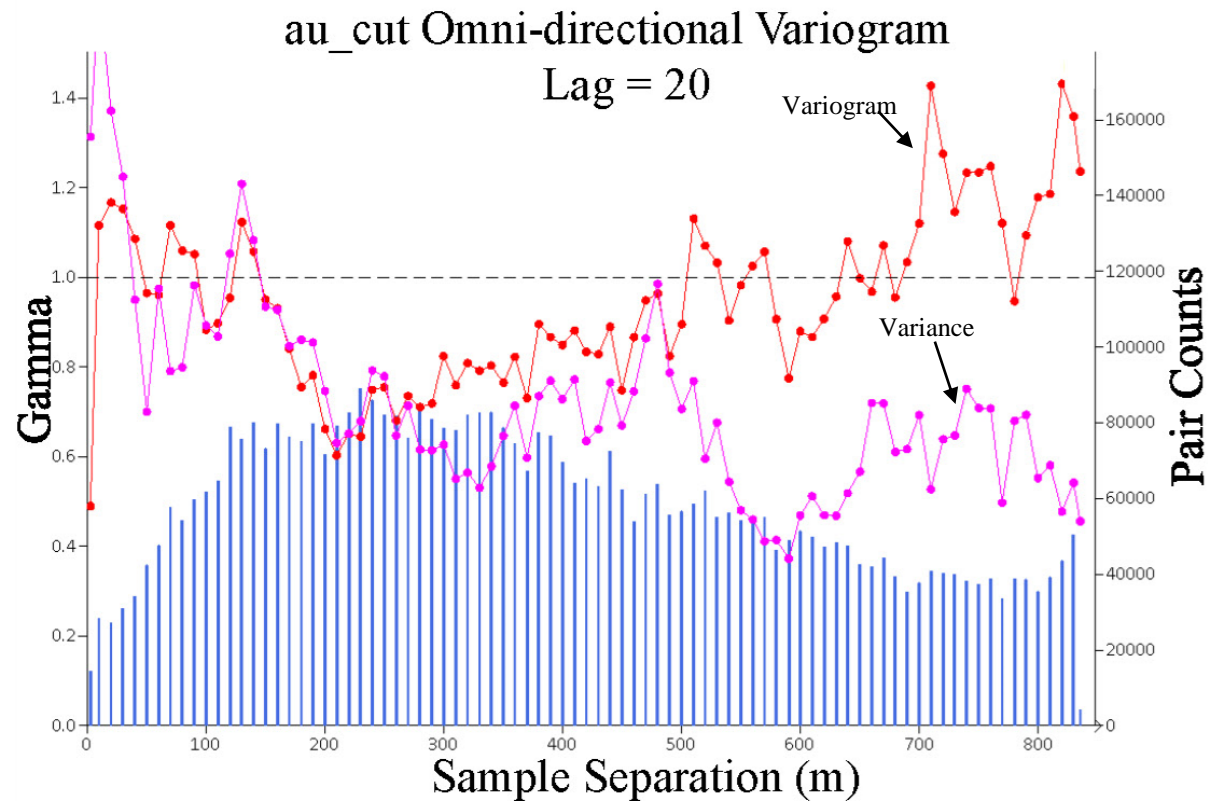
The change of sample composite length will also affect the robustness of variogram. In theory, the greater the composite length, the higher the smoothness of the samples, and the less the total number of samples used in the analysis of the variogram curve, which leads to the decrease of the contents of the curves and the gradual smoothing of the curve of the variogram. The smaller the composite length, and even the length is less than the global average sample length, the total number of samples will increase after the sample composited, and the amount of information of the variogram curve will increase, and more details of some original data will be considered to be generated, and then influence and even mislead the correct curve fitting. In order to research the influence extent of different composite length on the experimental variogram, the author re-composed 0.5m, 1m, 2m, 4m, 6m, 10m composite length for No. 1 ore body and No. 2 ore body, and try to analyze the relationship between the variation of the length of the composited sample and the structural characteristics of the variogram curve. All created variogram curves are as below Figure 4.

Through the comparison of the 6 groups of experimental variogram, with the increase of the composited sample length, the nuggets and sills of the variogram did not change obviously. Only when the composited length increased to 10m, a great change appeared in the curve, the value of nugget increased, the Sill level was flat, and the fluctuation amplitude decreased. It shows that the stability of the variogram will not produce substantial changes in a certain interval with the increase of the composited lengths. According to the composited sample length analysis, we can still choose 1m as the optimal composite length for this research project.



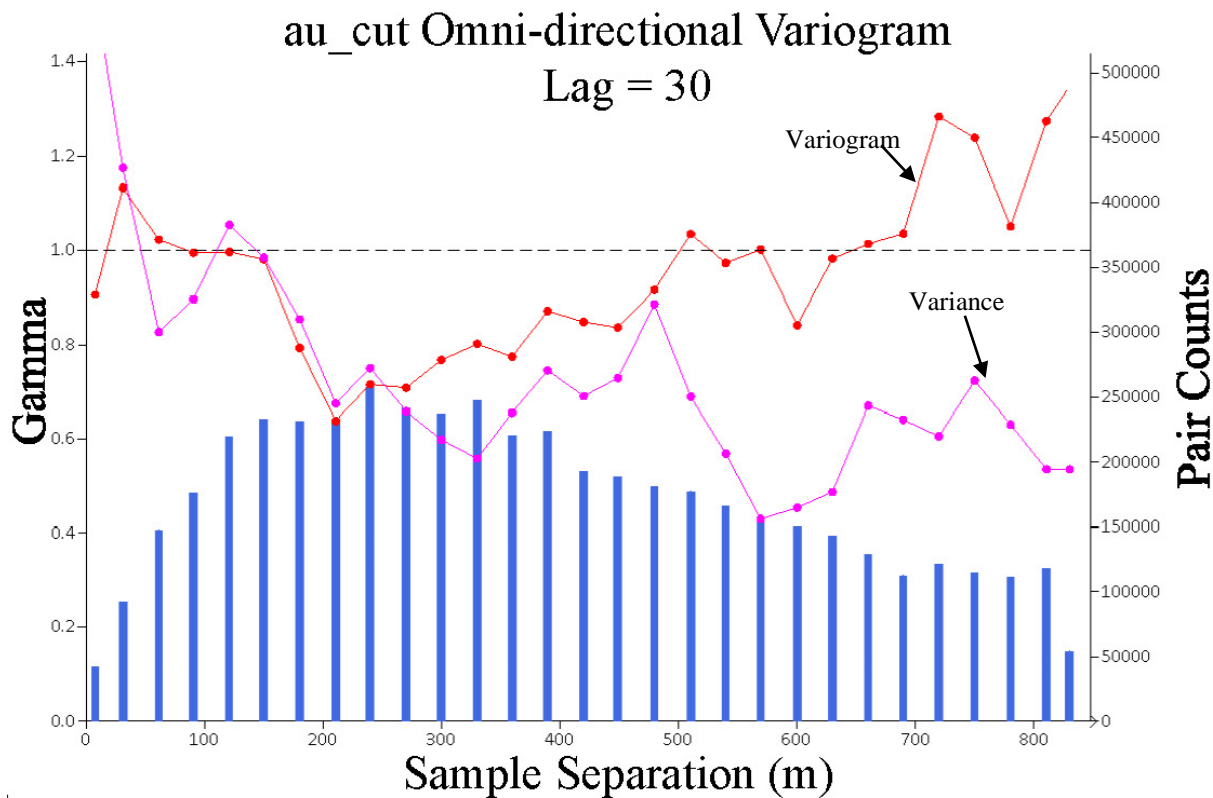
(1)

(1) Lag=10

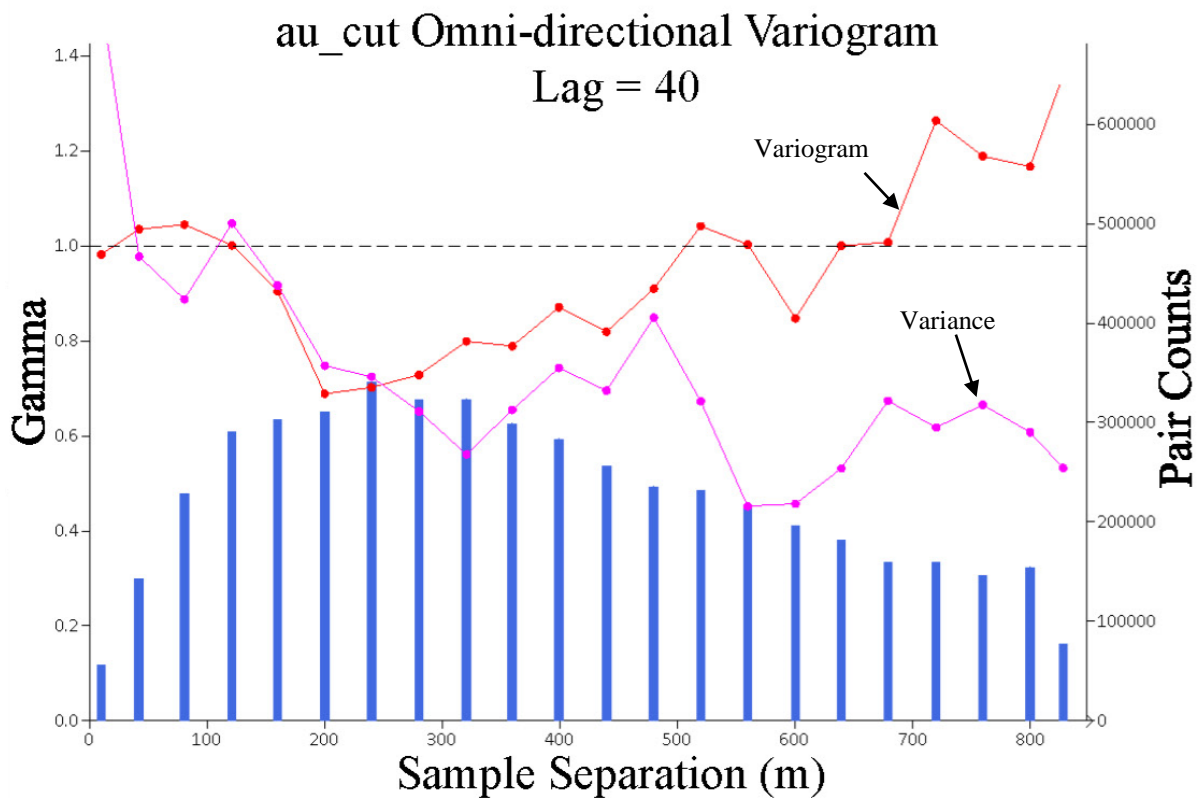


(2) Lag=20

Fig.2. Omidirectional Variogram by intervals (10m -100m intervals)

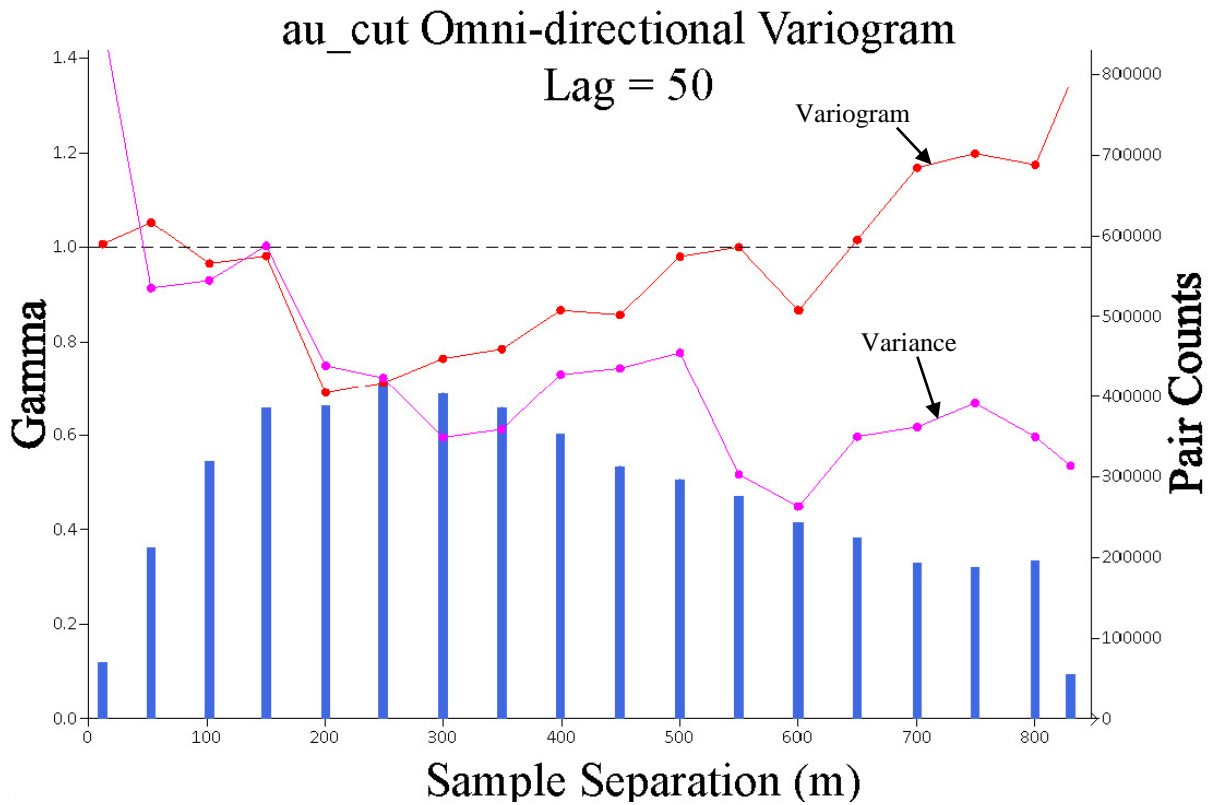


(3) Lag=30

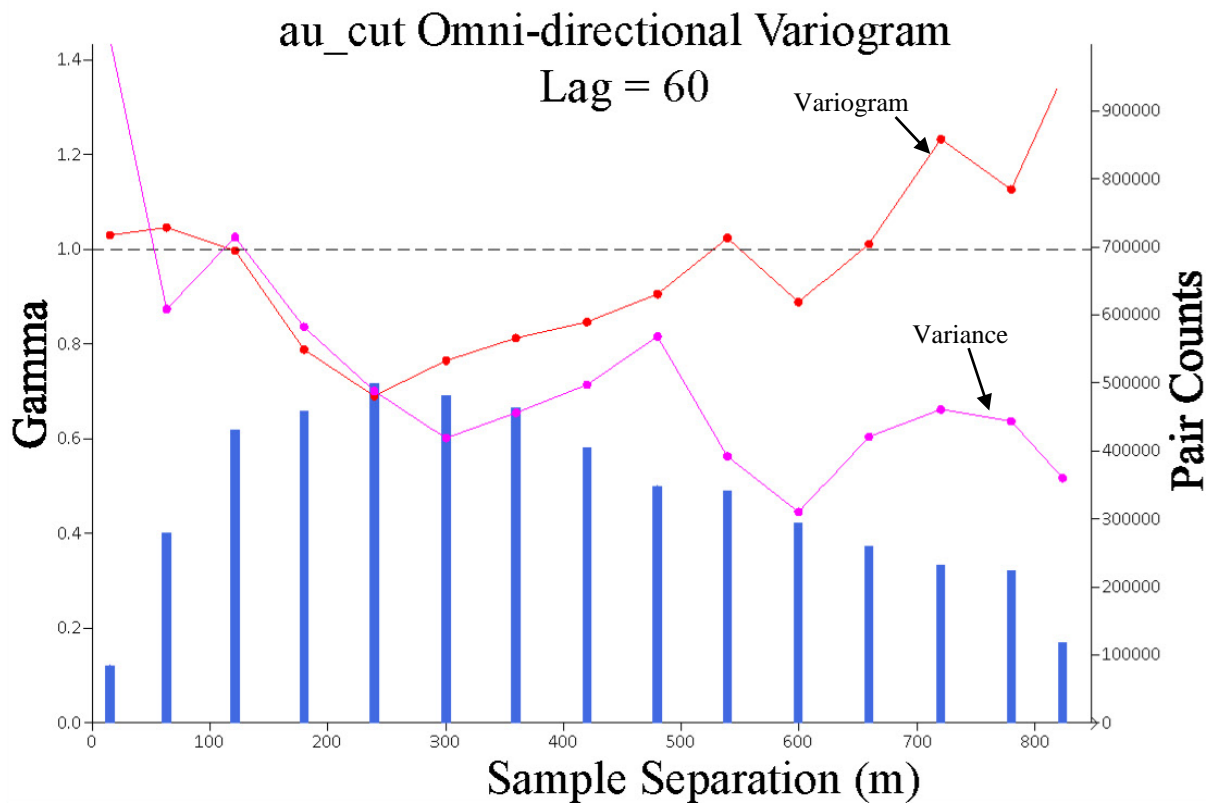


(4) Lag=40

Fig.2. Omidirectional Variogram by intervals (10m -100m intervals) continued

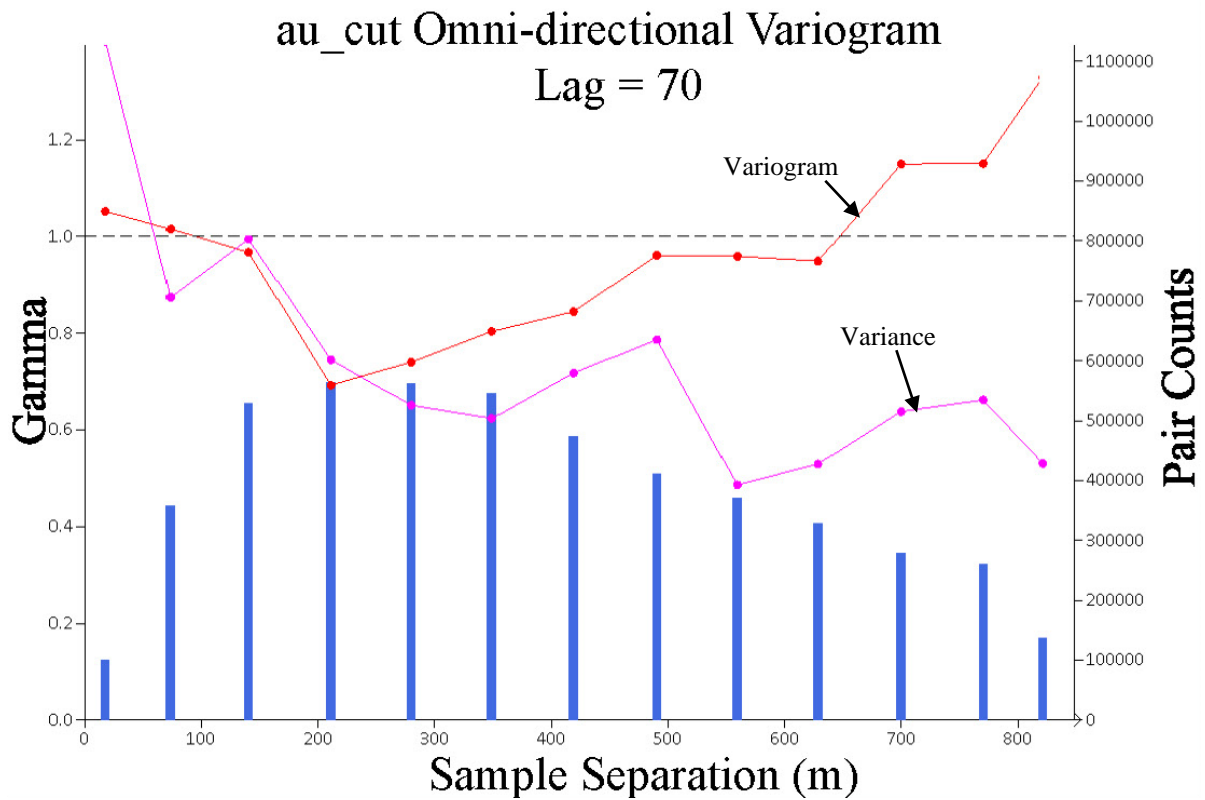


(5) Lag=50

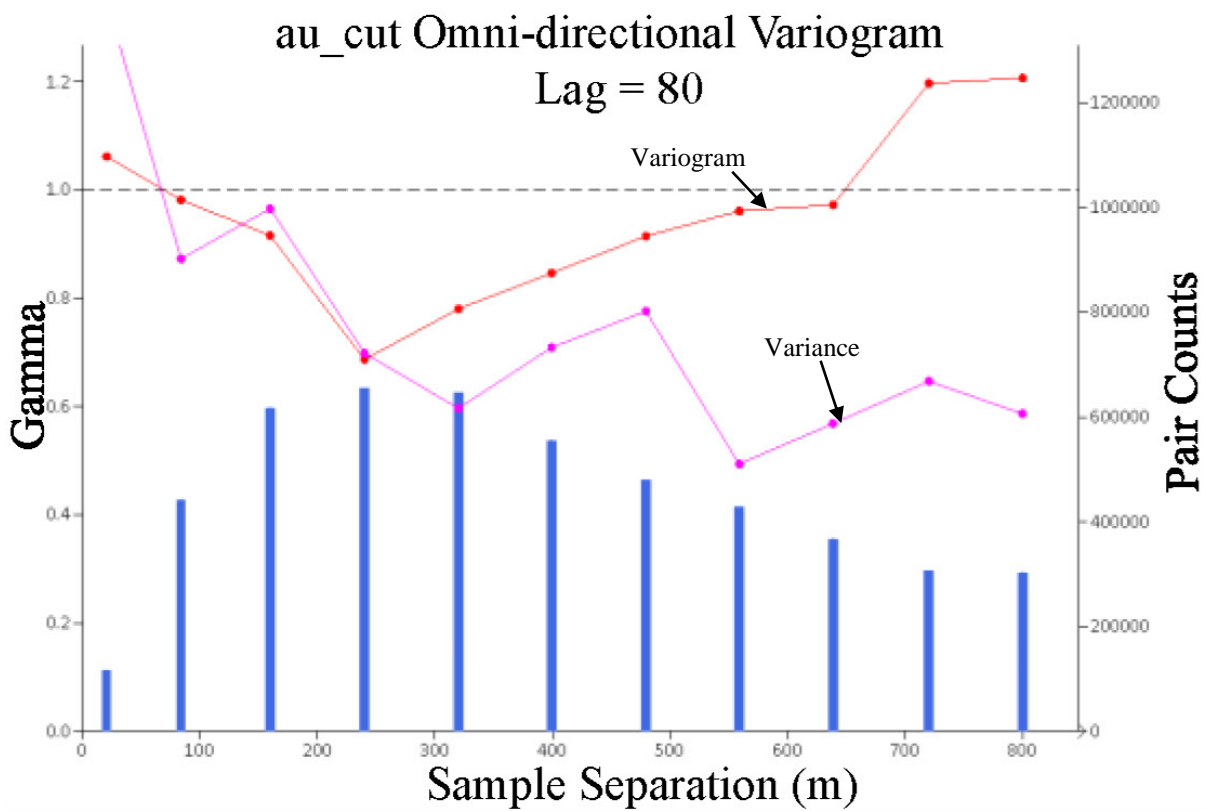


(6) Lag=60

Fig.2. Omidirectional Variogram by intervals (10m -100m intervals) continued

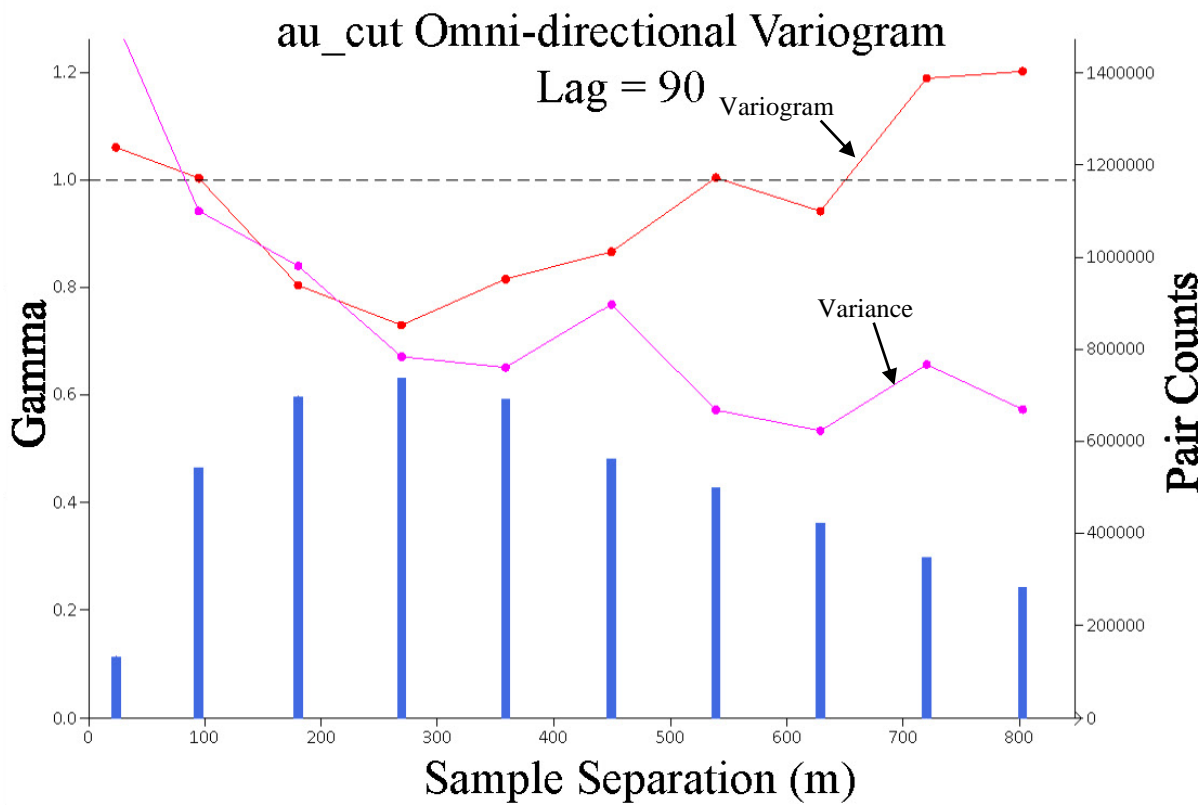


(7) Lag=70

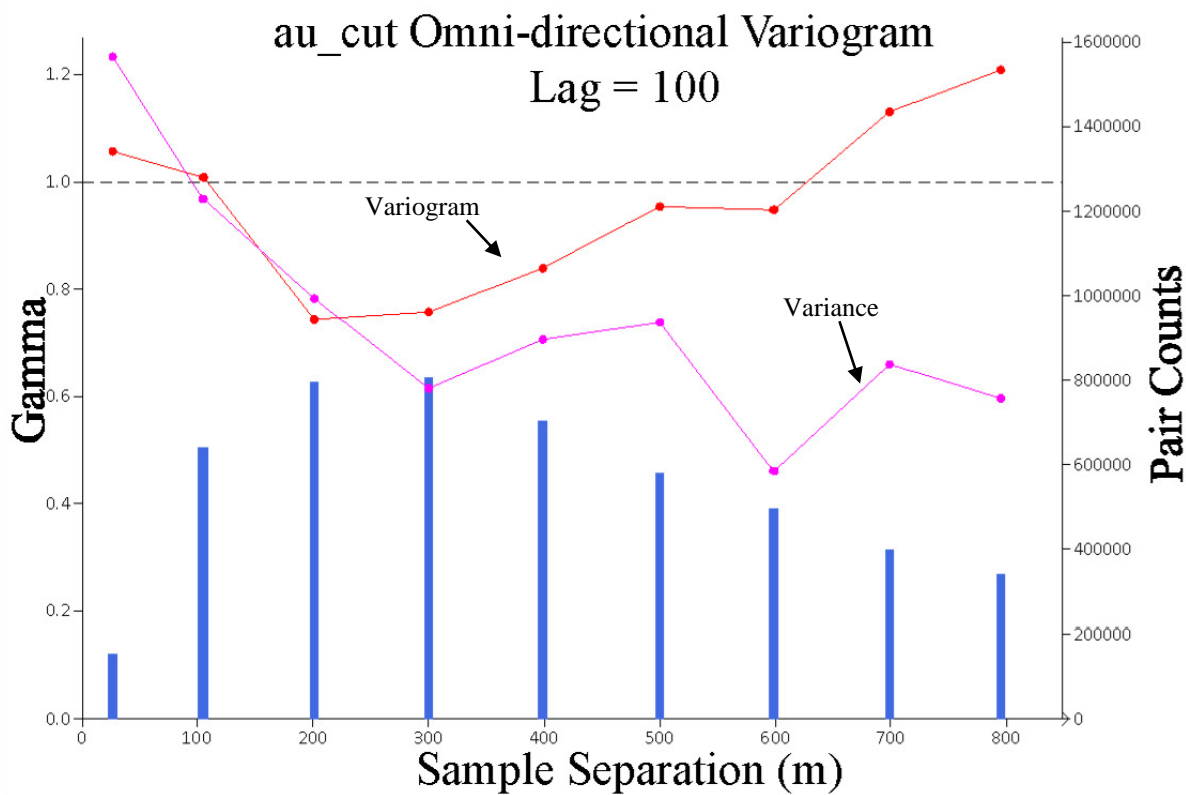


(8) Lag=80

Fig.2. Omidirectional Variogram by intervals (10m -100m intervals) continued



(9) Lag=90

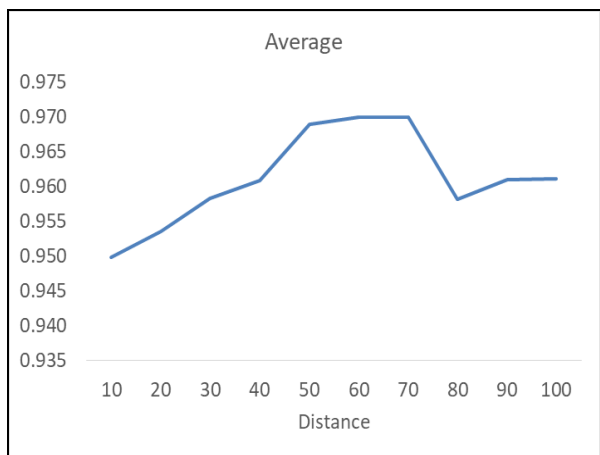


(10) Lag=100

Fig.2. Omidirectional Variogram by intervals (10m -100m intervals) continued

TABLE I .  
STATISTICS FOR VARIOGRAM (10m – 100m INTERVALS)

Interval	10	20	30	40	50	60	70	80	90	100
Average	0.950	0.953	0.958	0.961	0.969	0.970	0.970	0.958	0.961	0.961
Variance	0.036	0.033	0.032	0.032	0.032	0.034	0.032	0.025	0.026	0.026
Standard Deviation	0.189	0.180	0.179	0.178	0.179	0.183	0.178	0.158	0.160	0.161
Maximum value	1.430	1.400	1.350	1.360	1.350	1.370	1.330	1.210	1.200	1.210
Minimum value	0.490	0.630	0.640	0.690	0.690	0.690	0.690	0.690	0.730	0.740
Coefficient of Variance	0.199	0.189	0.187	0.185	0.185	0.189	0.184	0.165	0.166	0.167



(3-1) average trend curve

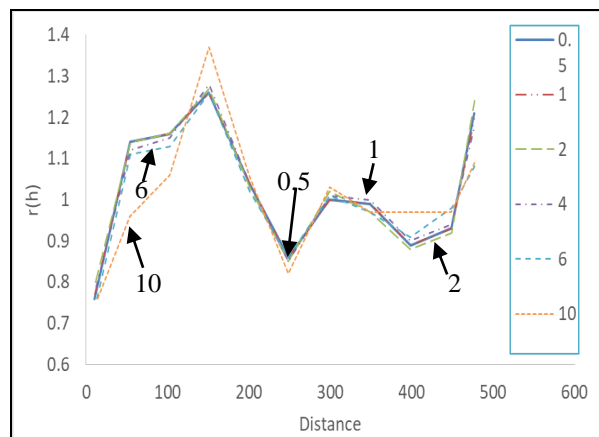
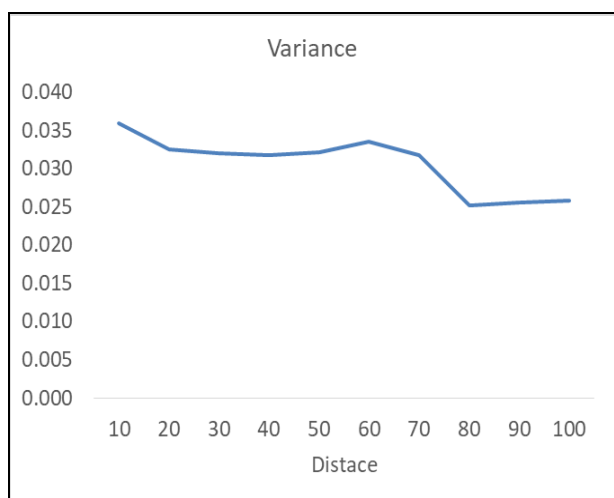
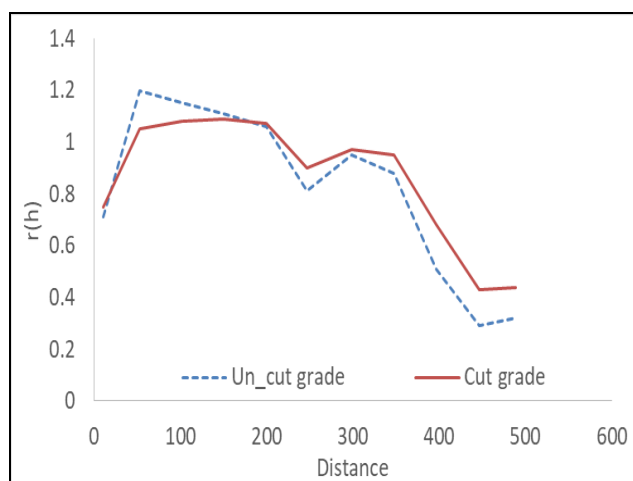


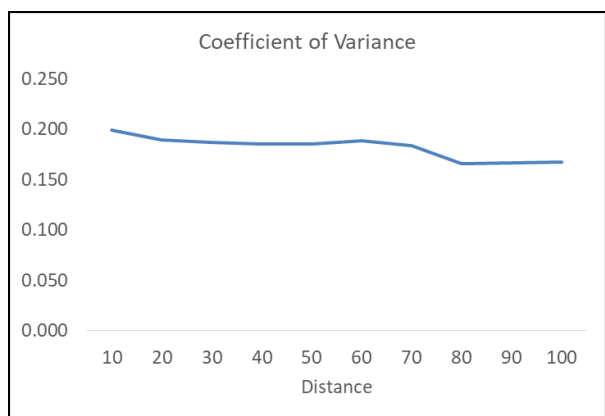
Fig.4. Variogram curves by composited lengths (0.5;1;2;4;6;10)



(3-2) variance trend curve

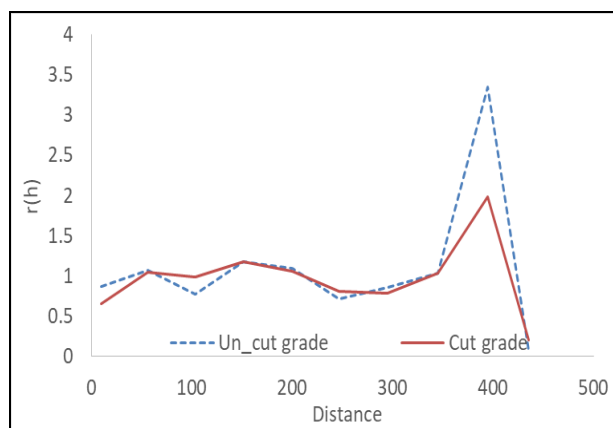


(5-1) ore body 1



(3-3) Coefficient of variance trend curve

Fig.3. Sampling interval variogram comparison



(5-2) ore body 2

Fig.5. Variogram curves by Top-cut

Taking the data of No. 1 and No. 2 ore bodies as an example, the comparison of the experimental variogram of the

mineralized data before and after the high grade treatment shows that before the top-cut of high grade outliers, the total variation of the mineralized data is stronger and the fluctuation of the variogram is very great, and the total variance of the data of No. 1 and No. 2 ore body is 0.1 and 0.72, respectively. The variance of the data is reduced to 0.06 and 0.2 after the high grade processing. The fluctuation of the data decreases significantly and the variogram becomes stable. The enhancement of the stability of the variogram is conducive to the structural analysis of the spatial variability of the data in the later stage and the correct fitting of the theoretical model.

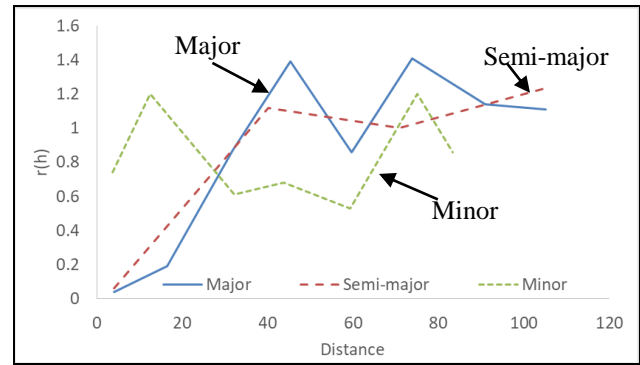
C. Analysis of proportional effect impact

The existence of proportional effect will increase the volatility of experimental variogram, increase nuggets and sills, and increase the estimation variance. The definition of proportional effect is as below:  $V(x_0)$  and  $V(x_0^1)$  are bistable regions whose centers are  $x_0$  and  $V(x_0)$  (such as  $V(x_0)$  representing the high grade mineralization region, and  $V(x_0^1)$  represents the low grade mineralization region),  $\gamma(h, x_0)$  and  $\gamma(h, x_0^1)$  are the corresponding variogram of the two regions. The two variograms have two averages  $m(x_0)$  and  $m(x_0^1)$  in the regions and  $V(x_0)$ , and the functions of the two averages are  $f[m(x_0)]$  and  $f[m(x_0^1)]$  which are proportional to each other and the ratio is  $\gamma_0(h)$ . The phenomenon is called as structural proportional effect, and the expression is as below:

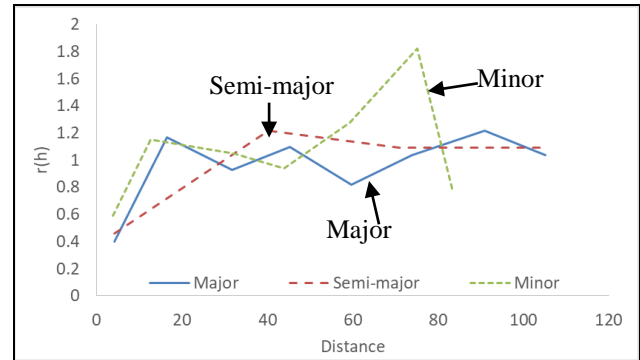
$$\frac{\gamma(h, x_0)}{f[m(x_0)]} = \frac{\gamma(h, x_0^1)}{f[m(x_0^1)]} = \gamma_0(h) \quad (2)$$

The following is the comparison of the variogram between the three directions of No. 1 ore body before logarithmic transformation and after logarithmic transformation.

It can be seen from the figures that before the logarithmic transformation of the data, the experimental variogram of the three directions are very different, and the value of the nuggets and the sills are very unstable, which is not conducive to the fitting of the later theoretical model. After the logarithmic transformation of the variogram, the nuggets of the three directional variogram is reduced to the acceptable range. With the increase of the distance, the sill values are gradually approaching to a relatively close stability value. The stability of the curve is significantly improved, which provides more convenience for the fitting model with better fitting degree.



(6-1) Original data



(6-2) Original data Logarithmic transformation data

Fig.6. Variogram curves by Proportional effect

Other potential impact factors which include mix-distribution impact, core recovery impact and drift effect impact were considered as sub impact factors, so these impact factors were not involved in the current stage analysis.

V. KRIGING MODEL NESTING AND STRUCTURE ANALYSIS

In order to facilitate the calculation, the variogram theoretical models used in the Kriging method of resource estimation are all isotropic, so it is necessary to convert them into isotropy when there is an anisotropic condition. The basic idea of transformation is to transform through linear transformation. When the initial coordinate vector is  $h = (h_u, h_v, h_w)^T$ , the initial coordinate vector does not need linear transformation under the isotropic condition [4-5].

A. Geometric anisotropic nesting

The geometric anisotropy model is different in the three directions of X, Y and Z. It needs to be transformed into a certain scale, and the geometric anisotropic model can be converted into an isotropic model. The concrete formulas are as below:

$$h_1 = \sqrt{\left(\frac{h_u}{a_u}\right)^2 + \left(\frac{h_v}{a_v}\right)^2 + \left(\frac{h_w}{a_w}\right)^2} \quad (3)$$

And the matrix format is:

$$A = \begin{Bmatrix} 1/a_u & 0 & 0 \\ 0 & 1/a_v & 0 \\ 0 & 0 & 1/a_w \end{Bmatrix} \quad (4)$$

The above assumption is based on the condition that three axes of ellipsoid are the same as original axes. Assuming that the three angles of the ellipsoid are azimuth angle  $\theta$ , dip

angle  $\phi$  and rotation angle  $\varphi$ , the rotation matrix is:

$$R = \begin{Bmatrix} \cos\varphi & 0 & -\sin\varphi \\ 0 & 1 & 0 \\ \sin\varphi & 0 & \cos\varphi \end{Bmatrix} \begin{Bmatrix} 1 & 0 & 0 \\ 0 & \cos\phi & -\sin\phi \\ 0 & \sin\phi & \cos\phi \end{Bmatrix} \begin{Bmatrix} \cos\theta & -\sin\theta & 0 \\ \sin\theta & \cos\theta & 0 \\ 0 & 0 & 1 \end{Bmatrix} \begin{Bmatrix} 1/a_u & 0 & 0 \\ 0 & 1/a_v & 0 \\ 0 & 0 & 1/a_w \end{Bmatrix} \quad (5)$$

In general, the geometric anisotropy model can be converted to isotropy through the above coordinate transformation.

**B. Zonal anisotropic nesting**

If both the distances and sills are different for different directions, it's called zonal anisotropy. The method of block processing is applied to zonal anisotropy, related process formula is as below:

$$\gamma(h) = w_1\gamma_1(h_1) + w_2\gamma_1(h_2) + w_3\gamma_1(h_3) \quad (6)$$

In the formula  $w_1$  is sill of major direction,  $w_1 + w_2$  is sill of semi-major direction,  $w_1 + w_3$  is sill of minor direction. And

$$h_1 = \sqrt{\left(\frac{h_u}{a_u}\right)^2 + \left(\frac{h_v}{a_v}\right)^2 + \left(\frac{h_w}{a_w}\right)^2}, h_2 = \frac{h_v}{a_v}, h_3 = \frac{h_w}{a_w}, \quad (7)$$

First, the three axes of the ellipsoid are converted to overlap with the three axis of the original coordinate system. The rotation matrix is the same as the matrix used in geometric anisotropy transformation, then the variogram  $\gamma_1(h_1)$ ,  $\gamma_2(h_2)$ ,  $\gamma_3(h_3)$  are generated according to the geometric anisotropic structure nesting. It is important to note that when the nested algorithm is used to generate the variogram of all directions, the change distances of the other two axes should be setting as enough large values, so that the current axial sill is only acting on the current axes.

Finally, the fitting results of the zonal anisotropic model are obtained by the above formula. Simply speaking, the zonal anisotropy is based on the geometric anisotropy, and superimposed processing was completed for extra sills of semi-major and minor directions.

Through the fitting of the exponential model, the theoretical fitting model of the three directions of No.1 ore body is obtained. The specific model expression is as below:

Major Direction:

$$\gamma(h) = \begin{cases} 0 & h = 0 \\ 0.05 + 0.95 \times (1 - e^{-\frac{h}{13.03}}) & h > 0 \end{cases} \quad (8)$$

Semi-major Direction:

$$\gamma(h) = \begin{cases} 0 & h = 0 \\ 0.05 + 0.95 \times (1 - e^{-\frac{h}{13.09}}) & h > 0 \end{cases} \quad (9)$$

Minor Direction:

$$\gamma(h) = \begin{cases} 0 & h = 0 \\ 0.05 + 0.95 \times (1 - e^{-\frac{h}{4.31}}) & h > 0 \end{cases} \quad (10)$$

The No.1 orebody is characterized by geometric anisotropy, and the sills of the three directions of the theoretical variogram are the same and the distances of variogram are different. The geometric anisotropy ratio of the three directions is 149:81.5:30.5=1:0.84:0.39, and the corresponding transformation matrix of the variogram is as below:

$$M = \begin{Bmatrix} 0.985 & 0 & 0.174 \\ 0 & 1 & 0 \\ -0.174 & 0 & 0.985 \end{Bmatrix} \begin{Bmatrix} 1 & 0 & 0 \\ 0 & 1 & 0 \\ 0 & 0 & 1 \end{Bmatrix} \begin{Bmatrix} 0.259 & -0.966 & 0 \\ 0.966 & 0.259 & 0 \\ 0 & 0 & 1 \end{Bmatrix} \begin{Bmatrix} 1 & 0 & 0 \\ 0 & 0.84 & 0 \\ 0 & 0 & 0.39 \end{Bmatrix} \begin{Bmatrix} 1 & 0 & 0 \\ 0 & 0.84 & 0 \\ 0 & 0 & 0.39 \end{Bmatrix}$$

Through the fitting of exponential model, the theoretical fitting model of the three directions of No.2 ore body is obtained. The specific model expression is as below:

Major Direction:

$$\gamma(h) = \begin{cases} 0 & h = 0 \\ 0.08 + 0.92 \times (1 - e^{-\frac{h}{45.42}}) & h > 0 \end{cases} \quad (11)$$

Semi-major Direction:

$$\gamma(h) = \begin{cases} 0 & h = 0 \\ 0.08 + 0.92 \times (1 - e^{-\frac{h}{37.98}}) & h > 0 \end{cases} \quad (12)$$

Minor direction:

$$\gamma(h) = \begin{cases} 0 & h = 0 \\ 0.08 + 0.92 \times (1 - e^{-\frac{h}{8.91}}) & h > 0 \end{cases} \quad (13)$$

The No.2 orebody is characterized by geometric anisotropy, and the sills of the three directions of the theoretical variogram are the same and the distances of variogram are different. The geometric anisotropy ratio of the three directions is 80:67.5:31.5=1:0.55:0.20, and the corresponding transformation matrix of the variogram is as below:

$$M = \begin{Bmatrix} 0.974 & 0 & -0.228 \\ 0 & 1 & 0 \\ 0.228 & 0 & 0.974 \end{Bmatrix} \begin{Bmatrix} 1 & 0 & 0 \\ 0 & 0.965 & 0.262 \\ 0 & 0.262 & 0.965 \end{Bmatrix} \begin{Bmatrix} 0.745 & -0.667 & 0 \\ 0.667 & 0.745 & 0 \\ 0 & 0 & 1 \end{Bmatrix} \begin{Bmatrix} 1 & 0 & 0 \\ 0 & 0.55 & 0 \\ 0 & 0 & 0.20 \end{Bmatrix} \quad (14)$$

**VI. ESTIMATION PARAMETERS OPTIMIZATION AND RESULTS**

After determination of variogram model fitting, there is still a large number of choices for use to make to optimize the next block model estimation stage and assess the kriging method performs.

It's clear that all measures should be made aiming to minimize mean squared error variance (kriging variance); however, if search parameters are not used condition of local stationarity will be not so important. In that case, other measures related to conditional bias and departure from theoretical optimality should be considered.

There are two major defined parameters can be used for assisting the determination of all estimation parameters such as block size, maximum samples, maximum sample per hole and discretization, etc.

1) The slope of regression is referring to the unknown true value of a random variable Z with estimation volume V against the known estimate of the random variable Z\* with the same volume V. The regression of the true values is an indication of the conditional bias in the estimate. The slope of regression approximates the conditional bias of the kriging estimation results.

If the fitting relationship curves between the original values and estimated values were Gaussian, the linear regression would be exactly the conditional expectation. Even if it's non-Gaussian, the slope of regression is still a reasonable approximated value of the conditional bias. The slope of regression is calculated as below equation:

$$SR = \frac{Cov(Z_v, Z_v^*)}{Var(Z_v^*)} = \frac{\sum_{i=1}^n \lambda_i \bar{C}(x_i, V)}{\sum_{i=1}^n \sum_{j=1}^n \lambda_i \lambda_j \bar{C}(x_i, x_j)} \quad (15)$$

The slope of regression for simple kriging is exactly 1. For other kriging methods as ordinary kriging where the Lagrange multiplier is used, the slope of regression is generally less than 1. Considering this, we could say that ordinary kriging is conditionally biased unless the slope of regression is equal to 1 (Lagrange multiplier is equal to 0).

2) Kriging efficiency was first developed by Krige (1997) as a measure tool of the efficiency of block estimates.

The kriging efficiency is expressed as the kriging variance ( $\sigma_{OK}^2$ ) normalized by the actual block variance as a percentage. We consider the estimates to be made on some volume V, and the corresponding variance of the blocks is equal to the average covariance between points within the blocks,  $\bar{C}(V, V)$  is defined as average values of covariance in the estimated volume V. We express kriging efficiency as KE with below equation:

$$KE = \frac{Var(Z_v^*) - Var(Z_v - Z_v^*)}{Var(Z_v^*)} = \frac{\bar{C}(V, V) - \sigma_{OK}^2}{\bar{C}(V, V)} \quad (16)$$

High efficiency values mean that the kriging variance is low, and the variance of the block estimates is approximately equal to the variance of the true block values. Low efficiency values indicate high kriging variance relative to the block variance. The kriging variance varies from block to block, so the kriging efficiency will vary as well.

For perfect valuations which were completed with enough original data, the efficiency is almost 100%. For all blocks were estimated with global mean, the KE will be 0. Besides above two conditions, most of time the KE values range from 0 to 1.

It's also noted that the Kriging efficiency can be negative if the kriging variance is greater than the block variance. When the estimation variance exceeds the block variance, Krige deems this a kriging anomaly and suggest to use mean for assignment assuming we know the accurate mean values [6-7].

### A. Block size Analysis

The choices of block size have direct impact for the estimation results. Oversized blocks cannot meet the requirements of different mineralizing characteristics and variability. The excessive smoothing of the ore grade distribution makes the variation function curve fitting and the search ellipsoid become negligible, the reducing of the fitting precision of the ore body boundary will be not useful for mining purposed pit optimization. The exploration and design of ore deposits and mine production planning will not be able to get any guidance from block model estimation. Undersized blocks can save more information including grade, lithology, distribution characteristics etc., but will lead to a decrease of the estimation accuracy [8-9], and undersized blocks which are much smaller than the selected minimum mining unit (SMU) will not be practical for mining industry. So

reasonable block sizes need be assessed and applied for resource and reserve estimation. When we use the minimum kriging variance as indicator for choice of block sizes, the selected block sizes are always much larger than the acceptable block sizes which can define the ore body boundary properly. The internal block variance should be considered as well, so the SR and KE are more suitable for the assessment of reasonable block size.

In this paper, 5m was selected as the Z axis block size and different X and Y arises block sizes were assigned for Kriging neighbor analysis. The above introduced parameter as SR and KE were plotted for the analysis process as below the figure:

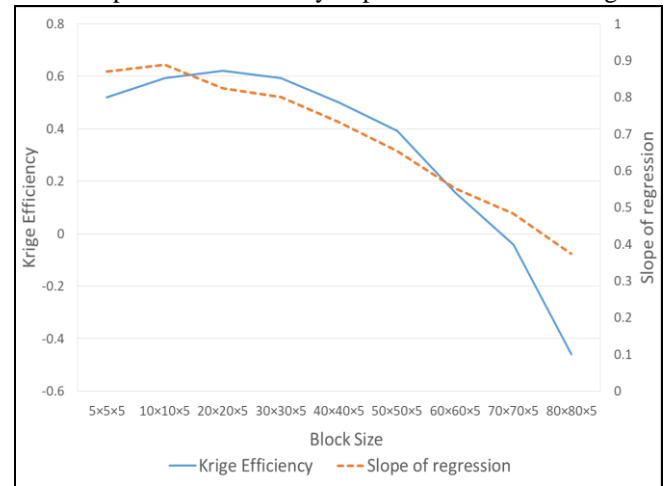


Fig.7. KNA analysis for X&Y block size

Based on above analysis figures, KE and SR inflection points were observed near the range form 20m × 20m to 30m × 30m which means all other block sizes will lead to worse estimation precision. In addition, taking the exploration spacing around 50m × 50m to 60m × 60m into account, the 30m × 30m was selected as the best block size.

Once the X and Y axis block sizes were confirmed, the 1,2,3,4,5m along Z axis plots were used for the analysis of Z axis direction block size assessment.

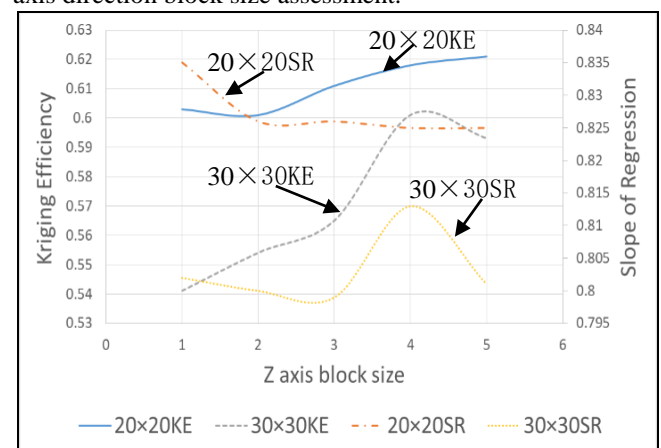


Fig.8. KNA analysis for Z block size

As we can see from the related figures, for 20m × 20m × (1-5m), the curves are gradually flat from 4m on, and for 30m × 30m × (1-5m), the maximum values for SR and KE all appears at 4m point from which we can make the conclusion that 30m × 30m × 4m is the best block size based on the KNA analysis.

**B. Maximum samples and maximum samples per hole**

Global simple kriging is the most statistically efficient unbiased linear estimator. But forcing the model to rely heavily on a strong global stationarity assumption is unrealistic in many cases. The reason of using Ordinary Kriging is to obtain a local estimate of the mean at the expense of introducing some conditional bias by limiting the search, and therefore reduce reliance on the assumption of a global stationarity mean throughout the whole domain.

Kriging with a more restrictive search domain will decrease the relative efficiency compared to kriging with a large search domain. The ratio of efficiencies would give a measure of how much variance is being incurred to decrease reliance on the global stationarity assumption. Ultimately, knowledge of how much the decision of stationarity could be relied upon would be necessary to determine an acceptable efficiency level.

Constraining the estimator will introduce a conditional bias. Constrained estimators are sometimes used in statistics because it is possible that an estimator with a small bias will have a smaller mean squared error (the mean squared error is equal to the variance plus the square of the bias).

In order to determine the proper maximum samples and maximum samples per holes to define the restricted domain. KE and SR parameters were extracted from 10 to 90 maximum samples (with 10 samples interval) for maximum samples analysis and 4,8,16 32 samples per hole for maximum samples per hole analysis.

slope of regression have the same develop tendency. A key finding of this plot is that as the number of search samples increases, the mean Kriging efficiency and slope of regression asymptotically approaches 1. This is because the estimator variances are approaching that of the theoretically best linear estimator: global simple kriging. What is observed for Krige’s efficiency, which plateaus is around 0.7. This is because the kriging variance is not being compared to the best possible case but to the block variance instead.

For the maximum samples plots, the increasing trends of KE indicate that the kriging variance gradually decreased. And the curve slope between 0 – 50 is much larger than the curve slope between 50 to 90 which implies flatter develop trend. Considering the raw data distribution density, 50 maximum sample should be selected as the optimized parameter which can also help to keep the overall variability if data distribution. For the maximum samples per holes, there is obvious inflection point was identified. The reason is: insufficient data with larger maximum samples per holes will lead to the situation that, all relative close samples which can be searched were included into the estimation process and the actual search domain shrunken than previous. Smaller search domain which is directly related to higher kriging variance and lower SR and KE. And based on different data distribution areas, the optimal parameter values must be changed. In current research case (The Shambesai main mineralized object 1), the inflection point appears at 8 samples per hole location which should be the optimal choice for the maximum samples per hole parameter.

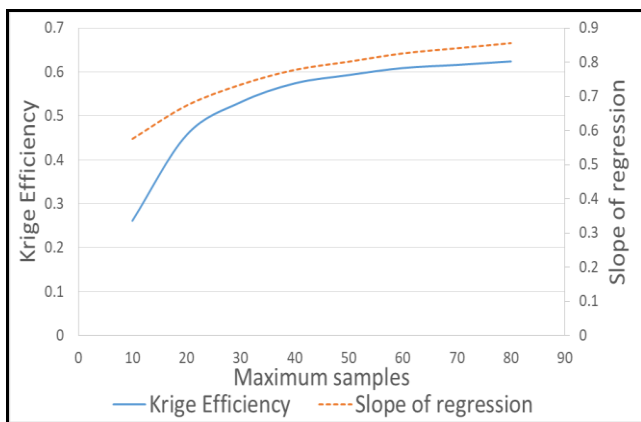
**C. Discretization**

The discretization coefficient in block model is mainly used to calculate the mean value of variogram or covariance. In the calculation process of the discretization coefficient, the principle is to divide the three axis direction of mother blocks into smaller block according to the system, and estimate each secondary block respectively. Finally, the average of all the parameters of the secondary blocks area calculated and reassigned as the value of original mother block. After the discretization computation is completed, all the secondary block parameters are removed from the temporary memory and will not be stored in the final model estimation results. The process of determining the discretization coefficient is to create a series of discretization coefficients and select reasonable discretization coefficients by calculating block covariance. For IDW estimation method, all the sub blocks are independent estimates, too large discrete coefficient will directly affect the estimation efficiency; and for Kriging estimation method, discretization coefficients are only used in covariance and block variance calculation with less impact, larger dimensions are also acceptable.

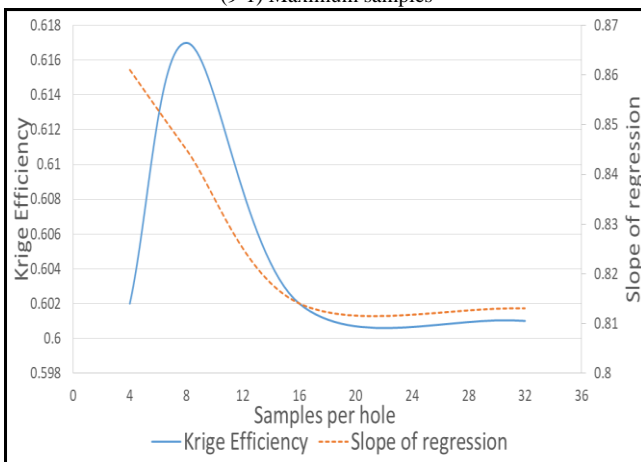
6 group of discretization coefficients were selected for analysis for the research, analysis results table and trend figures are as below Table II :

TABLE II.  
DISCRETIZATION COEFFICIENTS COMPARISON

Discretization	1×1×1	2×2×2	3×3×3	4×4×2	5×5×2	6×6×2
Block variance	10.23	3.283	2.746	2.703	2.653	2.628



(9-1) Maximum samples



(9-2) Maximum samples per hole

Fig.9. KNA analysis for samples

The analysis curve shapes of kriging efficiency and the

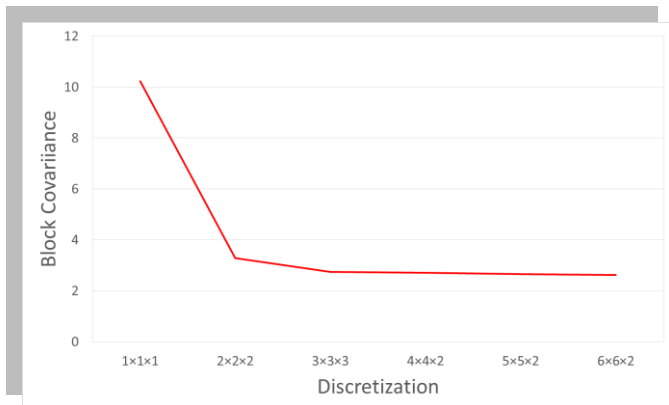


Fig.10. KNA analysis for discretization

The tables and figures show that the trend curve of block covariance from  $1 \times 1 \times 1$  to  $3 \times 3 \times 3$  interval include inflection point at  $3 \times 3 \times 3$  location, and the right side curve gradually tends to be gentle. Increasing the discrete coefficient dimension will no longer affect the block

covariance significantly. Therefore, the results show that the optimal discretization coefficient of  $3 \times 3 \times 3$  should be directly applied to the estimation of block models.

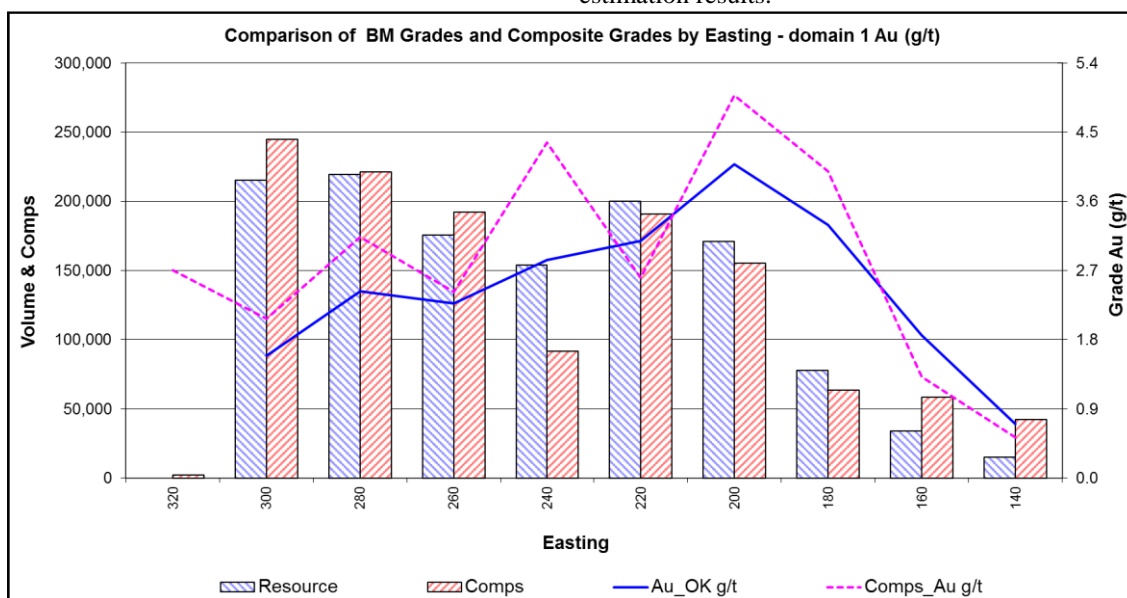
Final estimation results and validation process

After the experimental variogram impact factor analysis, the kriging nesting and structure analysis and the estimation parameter optimization, the ordinary kriging was performed for the resource estimation. The final estimation results were as below Table III:

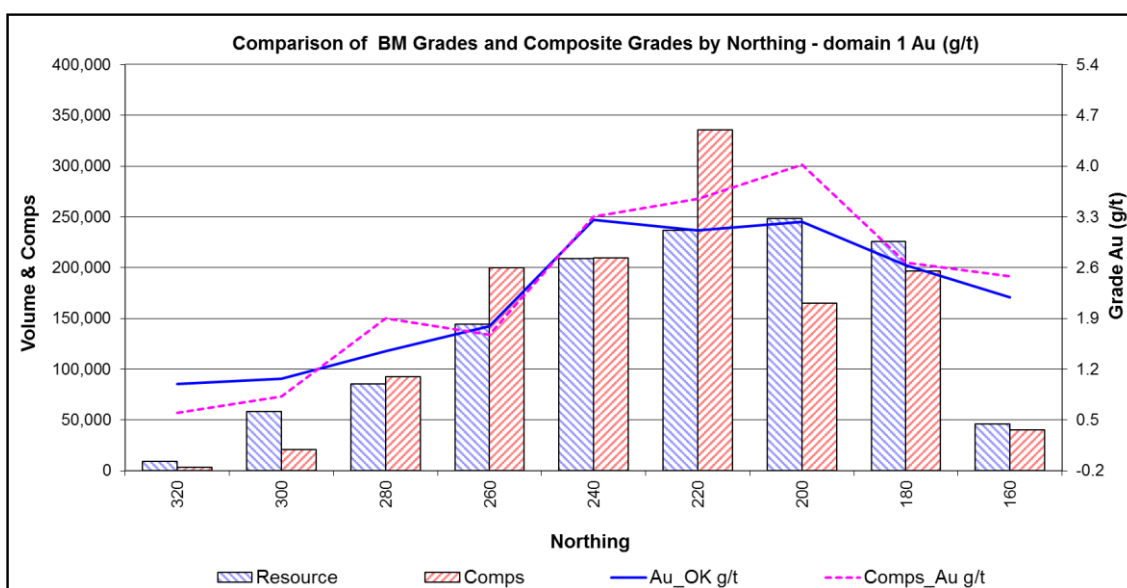
TABLE III  
RESOURCE ESTIMATION RESULTS

Gold grade range	Volume (m <sup>3</sup> )	Tones (t)	Au (g/t)	Au Metal (t)
< 0.2g/t	35,469	102,859	0.17	0.02
0.2 - 0.5 g/t	350,781	1,017,266	0.37	0.38
> 0.5 g/t	4,109,258	11,916,848	2.26	26.89
Total	4,495,508	13,036,973	2.09	27.28

The swats plots were created for the validation of the estimation results.



(11-1) Easting swats plot



(11-2) Northing swats plot

Fig.11. Swats plots for object 1&2 along X&Y axis

The 50m width banded areas were created for validation along X and Y direction. Based on the swats plot figures, the overall estimation grade distribution curves are highly correlate with original composite sample grades. In each local areas, estimated grades were reasonably smoothed to average value of previous higher and lower composite grades, interpolated estimation method was performed correctly [10-11]. Meanwhile, because the proper estimation parameters were applied, the impact estimation domains were constraint by the kriging parameters under proper extent, the typical local variabilities were still retained for the future efficient guiding of mining process.

## VII. CONCLUSION

1) Sampling spacing, top-cut, proportional effect and mixed distribution are the main effect factors of the stability of the experimental variogram of gold deposit data. With the increasing of the sampling spacing, the stability of the variogram is gradually increased, but the variability of the local area in the ore body is also gradually lost, so it is necessary to choose reasonable sampling spacing to balance the various aspects. The composite length does not cause substantial changes in a certain interval, but at the same time, the oversize composite length must not be selected. Top-cut is one of the most important factors that cause the decrease of stationarity of experimental variogram. It is suggested that proper top-cut be performed before variogram calculation. The existence of proportional effect will increase the volatility of experimental variogram, raise the nugget value and sill value, and increase the estimation variance. When the original data is not satisfied with the normal distribution, the logarithmic transformation of the data of the mining area is needed to obtain a more stable curve of the experimental variogram, which will greatly simplify the fitting process of the later variogram.

2) Supervisor geostatistical software was used to extract the nugget value in the directional variogram of the 1 and 2 ore bodies of the main ore body for the ore deposit, complete the fitting of the three direction variogram, and extract the parameters of the Kriging search ellipsoid. The fitting curve equation of variogram under the application of exponential model is calculated, and the corresponding transformation matrix is created for better estimation.

3) KNA analysis is carried out, with the parameters such as slope of regression (SR), Kriging efficiency (Kriging efficiency, KE) and covariance (Covariance, C0) as indicators. The parameter optimization for block model is completed. The optimal size of the block is 30 m×30 m×4 m, the optimal maximum sample number is 50, the optimum single hole sample number is 8, and the optimal discretization coefficient is 3×3×3. After parameter optimization, the relative error of the block estimation results of Kriging estimation and the original sample results is optimized, and the accuracy of the estimation is also improved.

4) The Ordinary Kriging estimation is completed, and the results are validated through the swats plot maps. The inverse distance power method has no variance constraints, but estimation with only considering of the distance in which the

anisotropy were ignored for local variability can be used when the data is insufficient and there is no major anisotropy continuity observed in the research areas.

## VIII. ACKNOWLEDGEMENTS

The research presented is partly supported by Research Start-up Fund for Introduced Talent of Kunming University of Science and Technology (Grant No. KKS201867017), which is greatly appreciated. Moreover, the authors would like to thank the anonymous reviewers for their valuable comments and constructive suggestions.

## REFERENCES

- [1] A. G. Journel, C. J. Huijbregts, "Mining Geostatistics [M]," New York, Academic Press, 1978.
- [2] G. Matheron, "Traité de géostatistique appliquée [M]," Paris, Technip, vol.ED-1, 1962.
- [3] G. Matheron, "Principles of geostatistics. Economic Geology [M]," vol. 58, pp. 1246–1266. 1963.
- [4] J. R. Hou, J. X. Huang, "Practical Geostatistics [M]," Beijing: Geological Press, 1998.
- [5] J. R. Hou, "Geostatistics (Special Information) Development and prospect [J]," *Geology and Exploration*, vol.1, pp. 53-58, 1997.
- [6] M. H. Manzurul, J. A. Peter, "Application of geostatistics with Indicator Kriging for analyzing spatial variability of groundwater arsenic concentrations in Southwest Bangladesh[J]," *Journal of Environmental Science and Health, Part A*, vol.11, pp. 1185-1196, 2011.
- [7] F. Rui, C. T. Paula, P. Lu's, "Application of indicator kriging to the complementary use of bio-indicators at three trophic levels [J]," *Environmental Pollution*, vol.157, pp. 2689-2696, 2009.
- [8] A. Naveed, L. Mohammed, "A Comparative Analysis of Time Coherent 3D Animation Reconstruction Methods from RGB-D Video Data [J]" *IAENG International Journal of Computer Science*, vol. 45, no.4, pp592-600, 2018
- [9] I. Seck, B. J. Van. "Geostatistical Merging of a Single-Polarized X-Band Weather Radar and a Sparse Rain Gauge Network over an Urban Catchment. [J]". *Atmosphere*, 9(12), 496, 2018
- [10] O. Karelin, A. Tarasenko, O. Barabash, M. Gonzalez-Hernandez, and J. Medina-Marin, "Modelling of Renewable Resource Systems with an Analysis of Changes of the Individual Parameter," *Lecture Notes in Engineering and Computer Science [J]" Proceedings of The World Congress on Engineering 2018*, 4-6 July, London, U.K., pp39-43, 2018
- [11] G. Lee, D. Kim, H. H. Kwon, and E. Choi, "Estimation of Maximum Daily Fresh Snow Accumulation Using an Artificial Neural Network Model [J]" *Advances in Meteorology*, 2019